An unusual space-time evolution for heavy ion collisions at high energies due to the QCD phase transition

D. Teaney and E.V. Shuryak
Department of Physics and Astronomy, State University of New York, Stony Brook, NY 11794-3800
(February 7, 2008)

The space-time evolution of high energy *non-central* heavy ion collisions is studied with relativistic hydrodynamics. The results are very sensitive to the Equation of State (EoS). For an EoS with the QCD phase transition, an unusual matter distribution develops. Before freeze-out, two *shells* are formed which physically separate and leave a maximum in the center. We make specific predictions for the azimuthal dependence of the flow and for two-pion interferometry, contrasting our results with a resonance gas EoS.

1. One of the principal goals of the heavy ion collision program is to find and to quantify the QCD phase transition from hadronic matter to a new phase, the quark-gluon plasma (QGP) [1]. Experiments at the Brookhaven AGS (lab energy 11 A*GeV) and at the CERN SPS (lab energy 200 A*GeV) are expected to produce a QGP/mixed phase during the initial stages of the collision, although currently there is only indirect evidence for this state (see the recent reviews [2]). With the completion of the Relativistic Heavy Ion Collider(RHIC) at Brookhaven and its much higher collision energy (100+100 GeV*A in the center of mass frame), the experiments are expected to produce the QGP well above the transition temperature. In this work, we study how the strong QGP pressure can be observed at RHIC.

The position-momentum correlations of the produced hadrons, colloquially known as collective *flow*, directly reflect the EoS of the excited matter. Multiple studies using cascade event generators and hydrodynamics (see e.g. [3–5]), have successfully reproduced the AGS/SPS hadronic spectra. A radial flow velocity of about (0.5-0.6)c is found in central PbPb collisions [2], but the flow develops principally during the late hadronic stages of the collisions and has little to do with the QGP. An EoS extracted from these model studies shows "softness" during the early stages of the collision, either due to the proximity of the QCD phase transition [5], or due to non-equilibrium phenomena such as the formation and fragmentation of strings [6].

2. Additional information about the EoS may be extracted from the azimuthal dependence of flow in *non-central collisions*, which depends non-trivially on the impact parameter and the collision energy. The ellipticity of the flow has been studied theoretically [7–10] and experimentally [11,12]. Because elliptic flow develops earlier than radial flow, its systematic measurement at the SPS may settle the mixed phase/pre-equilibrium controversy mentioned above. The original purpose of the present study was to further quantify elliptic flow within a hydrodynamic framework. Instead, we found that non-central collisions at RHIC/LHC energies have an unusual expansion pattern, which cannot be described as simply elliptic and which is qualitatively different from AGS/SPS energies.

3. Let us begin with a description of the transverse acceleration. In model calculations, the radial acceleration history changes from SPS to RHIC due to the QCD phase transition [13]. The ratio of pressure to energy density, p/ϵ, has a deep minimum at the end of the mixed phase, known as the "softest point" of the equation of state [14]. For AGS/SPS collision energies the matter is produced close to the softest point and the resulting transverse acceleration is small. Therefore, in non-central collisions the matter retains its initial elliptic shape and burns slowly inward. For RHIC/LHC collision energies, the early pressure starts an outward expansion [13]. This outward expansion and the inward deflagration can cancel each other, making a stationary front, called the "burning log" in [15]. Summarizing, at the AGS/SPS there is first softness and then a hadronic push, while at RHIC/LHC there is first a quark-gluon push, then softness, and then a hadronic push. In spite of this change, the final radial flow velocities at RHIC and at the SPS are expected to be similar [16].

4. The early push redistributes the matter, however. The early velocity has long time, $\sim 10 fm/c$, to influence the matter distribution before freeze-out. The stiff QGP in the center, with $T >> T_c$, pushes against the soft matter on the exterior, with $T \approx T_c$, producing a shell-like structure. Since the final distorted distribution rather resembles a nut and its shell, we call this picturesque configuration the *nutshell*. For high energy *non-central* collisions, the matter expands preferentially in the impact parameter direction (the x axis) and the expanding shells leave a rarefaction behind. Furthermore, since the acceleration started rather early, the two half-shells partially *separate*, and by freeze-out three distinct fireballs are actually produced. We have called this consequence of early pressure the *nutcracker* scenario.

5. Following [17,7], we assume a rapidity-independent longitudinal expansion. We then solve the 2+1 dimensional relativistic Euler equations in the transverse plane, with the coordinates x,y and proper time $\tau = (t^2 - z^2)^{1/2}$, using the HLLE Gudunov method [18]. As in previous calculations [14], we have used a simple bag model equation of state with $T_c = 160 MeV$ and a $1 GeV$ latent heat. We have modeled hadronic matter with a simple resonance gas EoS, $p = .2\epsilon$ [19]. The pressure was taken

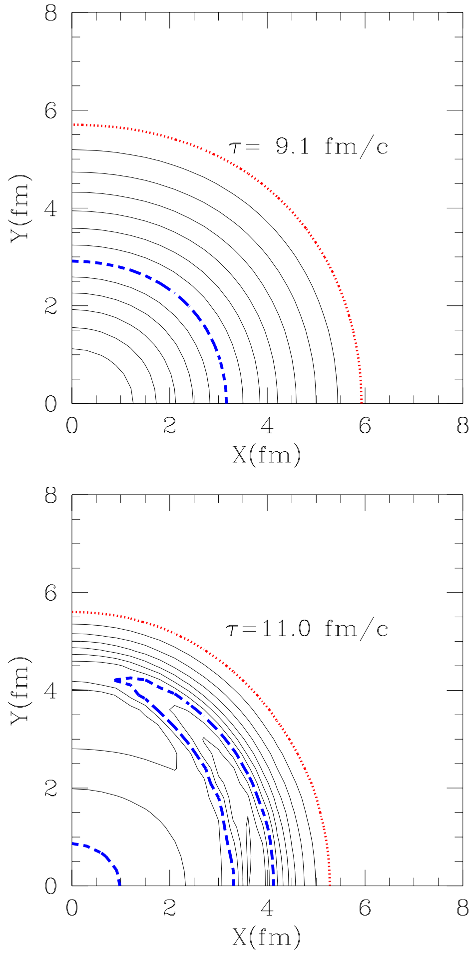

FIG. 1. Typical matter distributions in the transverse plane at mid rapidity, calculated using boost invariant hydrodynamics, for PbPb collisions at b=8 fm and proper time τ in a representative RHIC collision. For the corresponding central collision the pion multiplicity, including all isospin states, was $dN_\pi/dy = 850$. The outer dotted line and inner dashed line show temperatures of 120 and 140 MeV respectively. The solid lines show contours of constant energy density with a step size of 10 MeV. (a) shows the distribution at RHIC for a resonance gas EoS, p = $.2\epsilon$. (b) shows the distribution at RHIC for a bag model EoS.

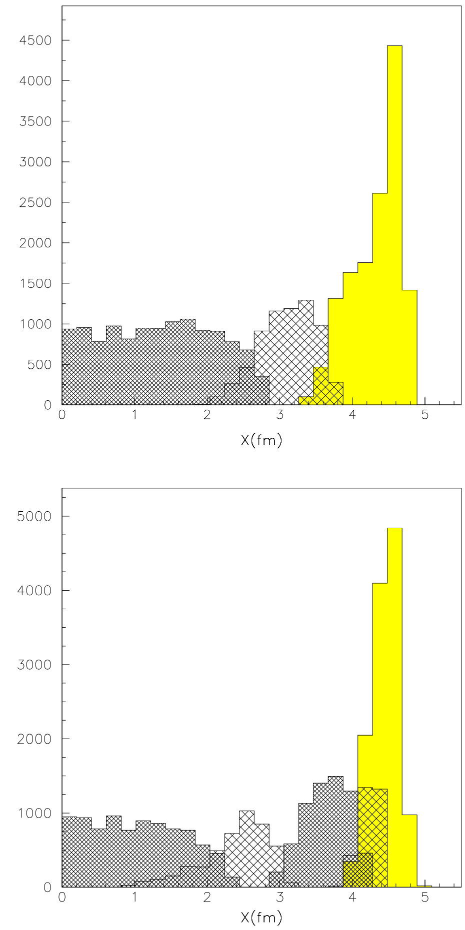

FIG. 2. The distribution (in arbitrary units) of the x coordinates of nucleons emitted from the spatial band, $|y| < 2fm$, and integrated over intervals of proper time. (a) shows the distribution for a resonance gas EoS. Grey, hatched and dark histograms are for $\tau < 8$, $8 < \tau < 9$ and $9 < \tau < (\tau_{max} = 10.5)$ fm/c , respectively. (b) shows the distribution for a bag model EoS. Grey, hatched and dark histograms are for $\tau < 10$, $10 < \tau < 11$ and $11 < \tau < (\tau_{max} = 12.5)$ fm/c, respectively.

to be independent of baryon number which is a good approximation at high energies. The initial entropy distribution in the transverse plane was assumed to be proportional to distribution of participating nucleons as in [7]. We parameterize the initial energy density by the total pion multiplicity, dN_π/dy. (How particle multiplicity maps to the collisions energy depends on the entropy production mechanism. This mapping will soon be determined experimentally at RHIC.) For definiteness, we consider PbPb collisions at an impact parameter of $b = 8fm$ and freeze-out at a fixed temperature, $T_f = 140MeV$.

At SPS energies the flow develops late, and the matter retains its initial almond shape until the late hadronic stage. However, at RHIC the flow develops early and redistributes the matter by late the hadronic stage. Two sample matter distributions, in the transverse plane and at fixed proper time, are shown in Fig. 1. A resonance gas EoS, $p = .2\epsilon$, produces little structure and simple elliptic flow (Fig. 1a). An ideal gas EoS, $p = \epsilon/3$, also produces simple elliptic flow and even shorter lifetimes (not shown). Finally, our bag model EoS produces two "nut-shells" of matter which expand outward (Fig. 1b). Note that in Fig. 1b the matter is pushed into two shells, moving in x direction, while at the north and south poles, two holes develop. A maximum, the "nut", remains in the center. The matter distribution becomes increasingly "nutty" with larger impact parameters and higher collision energies.

The evolution is clarified by plotting the emission points of nucleons, integrated over periods of proper time.

In Fig.2, (a) and (b), we show the x coordinates of the emitted nucleons for a resonance gas EoS and for a bag model EoS respectively. For both EoS, during the early stages, particles are slowly emitted from from a stationary freeze-out surface, making a peak at $x = 4 - 5$ fm [15]. For both EoS, however, 75% of the nucleons freeze-out during a short proper time interval of 2.5 fm/c. For a resonance gas EoS (Fig. 2a) the freeze-out positions are uniform and become increasingly centralized with time. In contrast, for a bag model EoS (Fig. 2b) the distribution has three distinct and comparable sources for the final 1.5 fm/c. There is a central "nut" and two extremal "shells" with a hole in between.

6. We turn now to the experimental consequences of this flow pattern. First we examine the ϕ distribution of the produced particles at mid-rapidity (y=0). These distributions are expanded in harmonics and are sometimes weighted by the transverse momentum squared.

$$\left.\frac{dN}{d\phi dy}\right|_{y=0} = \frac{v_0}{2\pi}(1+\sum_{n\geq 1} 2v_{2n}\cos(2n\,\phi)\,) \quad (1)$$

$$\int p_t^2 \left.\frac{dN}{dp_t d\phi dy}\right|_{y=0} dp_t = \frac{\alpha_0}{2\pi}(1+\sum_{n\geq 1} 2\alpha_{2n}\cos(2n\,\phi)\,) \quad (2)$$

We have calculated the single particle distributions for various secondaries, using the standard Cooper-Frye formula [20]. The elliptic components, v_2 and α_2, depend only weakly on collision energy, as found in previous studies [7]. For nucleons, for example, we found $v_2 \approx 7\%$ and $\alpha_2 \approx 13\%$ from the highest SPS energies to LHC energies.

Higher harmonics, in contrast, grow from SPS to RHIC. To summarize the effects of higher harmonics in the distributions, we have plotted in Fig. 3 the weighted net nucleon ϕ distribution (the l.h.s. of equation(2)) for SPS and RHIC, normalized to the first two terms in the Fourier expansions shown above. In the dashed curve corresponding to RHIC, the early pressure forces a $3-4\%$ additional asymmetry in final net nucleon distributions *beyond* the elliptic component. At LHC energies the additional asymmetry is even more pronounced. The marked minimum at 45^o is due to the square shape of the mater distribution, which somewhat reduces the flow on the diagonal. Note also a prominent positive correction to elliptic flow at 90^o. Both of these effects are observable, given the expected statistics at RHIC.

The distribution of deuterons and other heavy fragments should express the underlying flow more clearly. Because the emission points of the nucleons are bunched along the ridges of the nutshell, larger fragments are generally emitted from the shells. This inhomogeneity enhances the production probability of fragments and peaks their final flow in the x direction. Multiply strange barons such as Ω^- are also of interest. Since they do not rescatter in the hadron phase, they reflect the early flow [21]. Indeed any azimuthal dependence of the flow of multiply strange baryons would be fairly convincing evidence of collective motion in the quark phase.

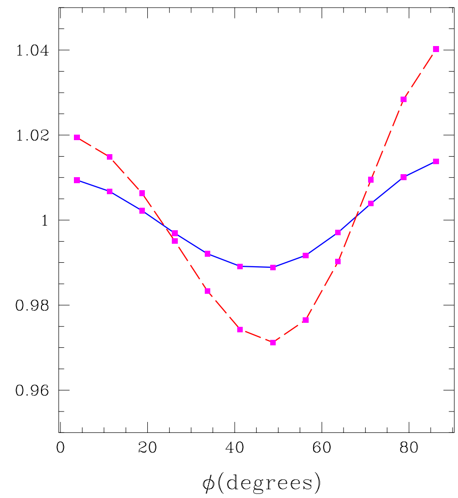

FIG. 3. The net nucleon ϕ distribution weighted by p_t^2 (the l.h.s. of equation(2)) and divided by the first two moments of the corresponding Fourier expansion (the r.h.s. of equation(2)). This plot summarizes the effect of all higher moments. The solid curve is for the SPS and the dashed curve is for RHIC. In the corresponding central SPS and RHIC collisions the pion multiplicity, including all isospin states, was $dN_\pi/dy = 525$ and $dN_\pi/dy = 850$ respectively. We summarize the numerical values below.
At the SPS : $< p_t^2 >=.67\ GeV^2$, $\alpha_2 = 12.0\%$, $\alpha_4 = 0.6\%$
At RHIC : $< p_t^2 >=.84\ GeV^2$, $\alpha_2 = 13.8\%$, $\alpha_4 = 1.3\%$
Note that α_0 is proportional to $< p_t^2 >$.

7. The *spatial* asymmetry of the matter distribution at freeze-out is probed by Hanbury Brown-Twiss (HBT) two particle interferometry. Strong flows strongly modify the source function. Each correlator with given pair momenta, is generated by its own "patch" , or "homogeneity region" [22]. Taking these patches together gives a complete picture of the source. We will discuss this complicated issue elsewhere, and here show only two selected correlators which emphasize the qualitatively different predictions of different EoS.

The correlators are found by taking the appropriate Fourier transform of the source function over the freeze-out surface [20]. Below we display the Hanbury Brown-Twiss(HBT) radii R_{xx} and R_{yy} and employ the notation $(p_1 + p_2)_\mu = 2K_\mu$ and $(p_1 - p_2)_\mu = q_\mu$. For R_{xx} we select $\vec{q}$ in the x direction , the direction we want to probe. $\vec{K}$ is chosen in the orthogonal y direction , with magnitude .5 GeV. For R_{yy} the axes of $\vec{K}$ and $\vec{q}$ are simply reversed. The correlators may then be fit to the functional form $C = 1 + exp(-q_i^2 R_{ii}^2)$, where R_{ii}^2 has been interpreted as the source size at zero velocity [23]. More specifically,

$$\begin{aligned} R_{xx}^2 &=< x^2 > - < x >^2 \\ R_{yy}^2 &=< y^2 > - < y >^2 \end{aligned} \quad (3)$$

These radii are shown in Fig. 4 for PbPb collisions at b=8 fm, as a function of the pion multiplicity scaled by the number of participants to central collisions (not b=8

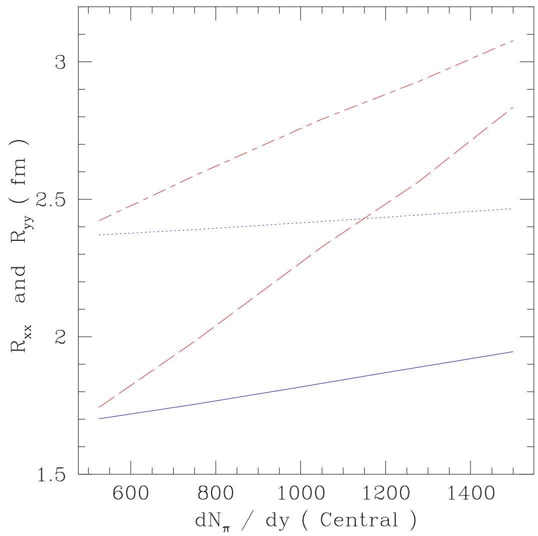

FIG. 4. HBT radii, R_{xx} and R_{yy} , for $|\vec{K}| = .5GeV$, as a function of the total pion multiplicity. The quoted multiplicity includes all isospin states and is scaled by the number of participants from b=8 fm to b=0 fm (a factor of 2.9) . See the text for more details. For a resonance gas EoS $p = .2\epsilon$, the solid lines and dotted lines show R_{xx} and R_{yy} respectively. For a bag model EoS, the dashed and dashed-dotted lines show R_{xx} and R_{yy} respectively.

fm). R_{xx} and R_{yy} are shown for a bag model EoS and for a simple resonance gas EoS, $p = .2\epsilon$. For low energies near the left hand side of the plot, the two EoS show approximately the same radii, roughly corresponding to the initial elliptic shape of the matter distribution. For a simple resonance gas EoS, the HBT Radii show little energy dependence, while for an EoS with the phase transition the homogeneity regions increase steadily with beam energy. The rapid increase of R_{xx} can be understood qualitatively. The contributing pions move in the y direction with rather high momenta, .5 GeV. The pair therefore originates, not from ridges of the nutshell, but from the region in between the shells. The rapid increase of R_{xx} reflects the increased separation of the nutshells at higher collision energies. The increase in R_{yy} reflects the flattening of the shells themselves. For flat, square-shaped, shells the homogeneity regions are larger than for curved elliptic shells.

8. In conclusion, for non-central heavy ion collisions, we predict an unusual space time evolution, which results from the interplay of a hard and soft EoS typical of the QCD phase transition. We have called this the "nutcracker" flow since two shells are produced and then separate. The azimuthal momentum asymmetry can be seen in the higher harmonics and flow of heavy secondaries, while the spatial asymmetry can be seen in HBT interferometry.

We end with the experimental strategy. As the "nutcracker" flow persists for all sufficiently non-central events, and because the principal RHIC detectors can determine the impact parameter plane, absolutely *any* observable, from strangeness, to flow, to J/ψ suppression, should display marked azimuthal dependence, which reflects the fireball in different stages. We urge our experimental colleagues to look for this dependence from the first day of operation at RHIC.

Acknowledgments. We thank J. Pons for essential numerical advice during the initial stages of this work and H. Sorge for many interesting discussions. This work is partially supported by US DOE, by the grant No. DE-FG02-88ER40388.

[1] E. Shuryak, Phys. Rep. **61**, 71(1980); Phys. Lett. **78B**, 150(1978); Sov. J. Nucl. Phys. **28**, 408(1978).
[2] R. Stock , hep-ph/9901415; S.A. Bass et al., J. Phys. **G25**, R1(1999).
[3] J. Sollfrank et al., Phys. Rev. **C55**, 392(1997).
[4] H. Sorge, Phys. Rev. **C52**, 3291(1995).
[5] C.M. Hung, and E. Shuryak, Phys. Rev. **C57**, 1891(1998).
[6] H. Sorge, Phys. Lett. **B402**, 251(1997).
[7] J.Y. Ollitrault, Phys. Rev. **D46**, 229(1992); Phys. Rev. **D48**, 1132(1993).
[8] H. Sorge, nucl-th/9812057 (1998).
[9] H. Sorge, Phys. Rev. Lett. **78**, 2309(1997).
[10] P. Danielewicz et al., Phys. Rev. Lett. **81**, 2438(1998).
[11] J. Barrette et al., (E877 Collaboration), Phys. Rev. Lett. **73**, 2532(1994).
C. Pinkenburg et al., (E895 Collaboration), nucl-ex/9903010.
[12] H. Appelshäuser et al., (Na49 Collaboration), Phys. Rev. Lett. **80**, 4137(1998).
[13] M. Kataja et al., Phys. Rev. **D34**, 2755(1986).
[14] C.M. Hung, E.V. Shuryak, Phys. Rev. Lett. **75**, 4003(1995).
[15] D. H. Rischke and M. Gyulassy, Nucl. Phys. **A608**, 479(1996).
[16] S. Bass, A. Dumitru, et al. , nucl-th/9902062.
[17] J.D. Bjorken, Phys. Rev. **D27**, 140(1980).
[18] V. Schneider et al., J. Comput. Phys. **105**, 92(1993).
For more powerful high resolution methods see:
J. Pons et al., Astron. & Astrophy **339**, 638(1998).
F. Eulderink and G. Mellema, Astron. & Astrophy. Suppl. Ser **110**, 587(1995).
[19] E. Shuryak, Sov. J. of Nucl. Phys. **16**, 395(1972); R. Venugopalan and M. Prakash, Nucl. Phys. **A546**, 718 (1992).
[20] F. Cooper and G. Frye, Phys. Rev. **D10**, 186(1974);
F. Cooper, G. Frye, E. Schonberg, Phys. Rev. **D11**, 192(1975).
[21] H. Sorge, Phys. Rev. Lett. **81**, 5764(1998).
[22] A.N. Makhlin and Yu.M. Sinyukov, Z. Phys. **C39**, 69(1988).
[23] U. Heinz and B.V. Jacak, prepared for Ann. Rev. Nucl. Part. Sci, **49**(1999) .